An analytical model of a longitudinal-torsional ultrasonic transducer

Hassan Al-Budairi, Margaret Lucas

School of Engineering, University of Glasgow, Glasgow, G12 8QQ, UK

h.al-budairi.1@research.gla.ac.uk, Margaret.Lucas@glasgow.ac.uk

Abstract. The combination of longitudinal and torsional (LT) vibrations at high frequencies finds many applications such as ultrasonic drilling, ultrasonic welding, and ultrasonic motors. The LT mode can be obtained by modifications to the design of a standard bolted Langevin ultrasonic transducer driven by an axially poled piezoceramic stack, by a technique that degenerates the longitudinal mode to an LT motion by a geometrical alteration of the wave path. The transducer design is developed and optimised through numerical modelling which can represent the geometry and mechanical properties of the transducer and its vibration response to an electrical input applied across the piezoceramic stack. However, although these models can allow accurate descriptions of the mechanical behaviour, they do not generally provide adequate insights into the electrical characteristics of the transducer. In this work, an analytical model is developed to present the LT transducer based on the equivalent circuit method. This model can represent both the mechanical and electrical aspects and is used to extract many of the design parameters, such as resonance and anti-resonance frequencies, the impedance spectra and the coupling coefficient of the transducer. The validity of the analytical model is demonstrated by close agreement with experimental results.

1. Introduction

Improvement in ultrasonic transducer performance requires a detailed investigation of the mechanical and electrical characteristics for different operating conditions. It is also important to simulate the effects of the mechanical, dielectric and piezoelectric losses which are associated with the transducer, prior to fabrication. For instance, numerical modelling based on the finite element (FE) method allows for an accurate description of the mechanical behaviour where the stresses and strains can be calculated accurately, but does not generally provide adequate insights into the electrical characteristics. Numerical modelling also requires large computational power and sometimes, due to the numerical characterisation, the physical meaning of the model may be lost [1]. Therefore, involving the optimized numerical model directly in the fabrication stage can lead to a mismatch between the actual and the expected performance.

The analytical model of wave motion is used as an alternative method to design piezoelectric transducers which is based on the solution of the wave equation along the transducer. It is generally used in one-dimensional vibration theory where the longitudinal dimension of the transducer is greater than the lateral dimension and therefore only the longitudinal modes are considered [2]. Analytical approaches can also be applied in two-dimensional and three-dimensional models to consider flexural, radial and longitudinal modes of vibration [3], requiring more advanced mathematics for solution. In the current work, a 1D model is modified to represent an optimised design of an LT transducer where the design optimisation has been presented in previous work [4]. The developed 1D model has the

following advantages: it is simple to model; it can be used to investigate the electrical characteristics of the transducer by calculating the electrical impedance, the phase diagram, and the coupling coefficient; it is possible to model the effects of mechanical and electrical losses of the piezoelectric and acoustic elements of the transducer [5]; it can be used to calculate the input electrical power and the output mechanical response for different excitation levels; and, finally, it is possible to create a mode shape by calculating the currents of the equivalent network branches, the mode shape being important for locating the nodal plane of the transducer.

2. Mason equivalent circuit model

Mason's model provides a powerful tool for the analysis and simulation of piezoelectric transducer elements. This model simulates both the coupling between the mechanical and electrical systems and the coupling between the mechanical and acoustical systems [6]. The equivalent circuits of piezoelectric and acoustic materials are shown in Figure 1, where the force, f_i, and velocity, v_i, are represented by an electric potential, V_{mi}, and current, I_{mi}, respectively, the acoustic impedance of these materials is represented by electrical capacitance, Z_C, and inductance, Z_L, elements, and these elements are calculated from the material properties as follows:

$$Z_L = j\,\rho\,c\,S\,tan(\frac{k\,l}{2}) \tag{1}$$

$$Z_C = \frac{-j\,\rho\,c\,S}{sin(kl)} \tag{2}$$

Where ρ,c,S,k and l are the material density, the sound velocity, the cross-sectional area, the wave number and the wave path length in the direction of wave propagation respectively.

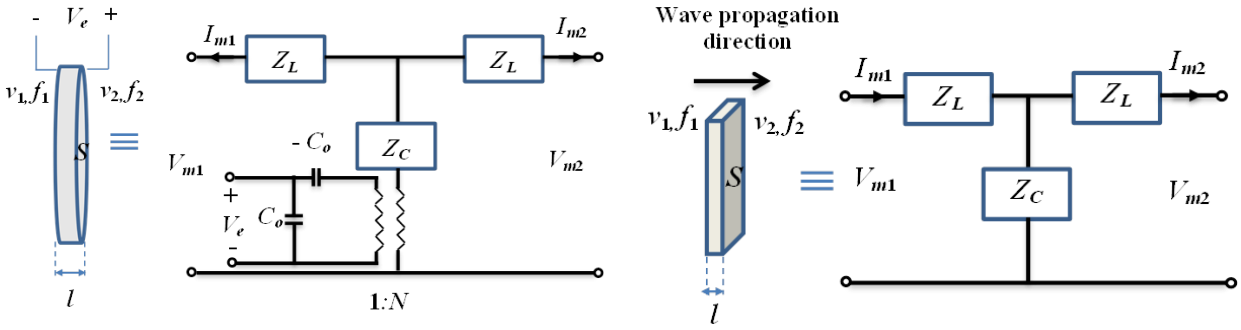

Figure 1. Mason equivalent circuit of a piezoelectric disc (left) and an acoustic solid (right).

3. Analytical model

The schematic of an LT transducer model is shown in Figure 2. The construction of the equivalent circuit is carried out by dividing the model into six regions where there are changes in material, cross-sectional dimensions, or both between these regions. After defining the material properties and the geometrical dimensions, equations (1) and (2) are used to calculate the inductance and capacitance impedances as functions of frequency for each region.

As shown in Figure 2, regions 2 and 3 are composite structures of different parts, region 2 has a hollow back mass and a bolt through the back mass and region 3 has piezoceramic disks, electrodes, and the bolt through the disks. In order to consider the acoustical effect of the bolt, the average values of the material properties of these regions are considered [7]. Region 5 represents the slotted helical geometry of the front mass, where this complex structure has an inner uniform solid core and an outer exponential slotted profile as shown in Figure 3(a). The force, F, generated at the piezoelectric disks region remains constant along the uniform section of region 4 and then divides at the slotted region 5 into two components: longitudinal force, F_L, and shear force, F_T, which can be expressed as;

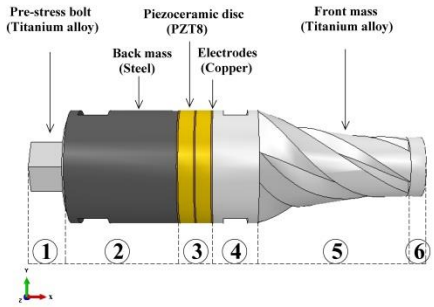

Figure 2. Exploded schematic of the LT transducer.

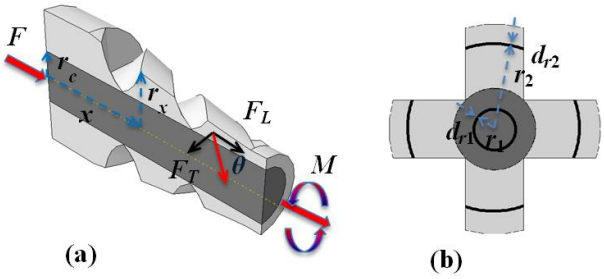

Figure 3. (a) Section of the exponential slotted front mass **(b)** cross-section normal to the wave motion.

$$F_L = F\ cos(\theta) \tag{3}$$

$$F_T = F\ sin(\theta) \tag{4}$$

where θ is the helix angle of the slots.

Based on the theory of longitudinal and flexural vibration, the longitudinal force component will create longitudinal vibration, while the shearing force component will create torsional vibration [8]. The shearing component produces a torsional moment, *M*, along the axis of the horn which can be expressed as;

$$M = \int r\ f\ dS \tag{5}$$

Where *f* is the shearing force acting on a unit area, *dS*, at radius, *r*.

The cross-sectional area of this region is a combination of slotted and solid core areas, as shown in Figure 3(b), which can be found as:

$$S_1 = \pi\ r_1^2 \qquad for \qquad 0 < r_1 \leq r_c \tag{6}$$

$$S_2 = \pi\ r_2^2 - \pi(r_2 - r_c)^2 \qquad for \qquad r_c < r_2 \leq r_x \tag{7}$$

Differentiating equations (6) and (7), so that;

$$dS_1 = 2\pi\ r_1 dr_1 \tag{8}$$

$$dS_2 = 2\pi\ r_c dr_2 \tag{9}$$

Applying equations (8) and (9) into equation (5);

$$M = \int_0^{r_c} r_1\ \frac{F\ sin(\theta)}{\pi\ r_1^2}\ 2\pi r_1 dr_1 + \int_{r_c}^{r_x} r_2\ \frac{F\ sin(\theta)}{2\pi\ r_c r_2 - \pi r_c^2}\ 2\pi\ r_c dr_2 \tag{10}$$

The simplified equation is then;

$$M = 2F\ sin(\theta)\ [\int_0^{r_c} dr_1\ + \int_{r_c}^{r_x} \frac{r_2 dr_2}{2r_2 - r_c}] \tag{11}$$

We have;

$$\int \frac{x\ dx}{ax + b} = \frac{x}{a} - \frac{b}{a^2} ln|ax + b| \tag{12}$$

From equation (11), it could be found that (a = 2) and (b = -r_c), by applying the integration solution, the shear moment equation will be;

$$M = 2F\,sin(\theta)\,[\frac{r_c}{2} - \frac{r_c}{4}\,ln|r_c| + \frac{r_x}{2} + \frac{r_c}{4}ln|2r_x - r_c|] \tag{13}$$

The equivalent circuit of region 5 can then be obtained by two separate circuits of the 1D model, the first circuit representing the longitudinal vibration component and the other circuit representing the torsional vibration component. Each circuit interacts with region 4 through a conversion coefficient which is the ratio of degenerated vibration to the generated vibration at the dividing surface (output of region 4). The conversion coefficient of longitudinal vibration, n_L, and torsional vibration, n_T, are given by;

$$n_L = \frac{F_L}{F} \tag{14}$$

$$n_T = \frac{M}{F} \tag{15}$$

Applying equations (3) and (13) in equations (14) and (15) respectively, gives;

$$n_L = cos(\theta) \tag{16}$$

$$n_T = 2\,sin(\theta)\,[\frac{r_c}{2} - \frac{r_c}{4}\,ln|r_c| + \frac{r_x}{2} + \frac{r_c}{4}ln|2r_x - r_c|] \tag{17}$$

The complete equivalent network of the transducer is shown in Figure 4, where two more impedances are added at both end sides of the circuit which represent the front, $Z_{front\ L}$ and $Z_{front\ T}$, and back, Z_{back}, external loads. These impedances are neglected when the transducer is tested under free conditions (unloaded) because they represent the surrounding space impedance which has a small value, but when the transducer is tested under operational load, their values should be considered.

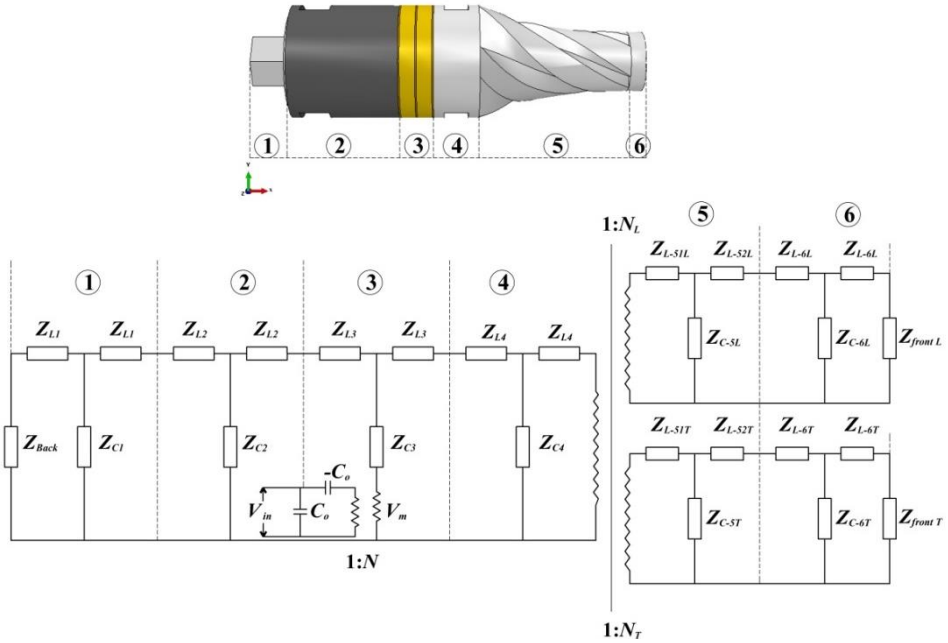

Figure 4. A complete equivalent network of the LT transducer.

4. Results

A Mathematica program is created to solve the complete equivalent circuit and extract the resonance and anti-resonance frequencies, the coupling coefficient and the ratio of torsional to longitudinal response at the output surface. The results are compared to experimental results as shown in Table 1;
There is an excellent match between the frequency values and a good agreement of the response ratio, but, the difference in the coupling coefficient values may relate to a difference in the piezoelectric constant, d_{33}, due to the application of pre-stress, which is not considered in the analytical model.

Table 1. Comparison of analytical and experimental results.

	Resonance f_r (Hz)	Anti-resonance f_a (Hz)	Coupling Coefficient k_{eff}	T/L response
Analytical	19,451	19,706	0.16	0.64
Experimental	19,426	19,886	0.20	0.59
% diff.	0.1%	0.9%	20%	8%

The electrical impedance and the phase diagram are calculated and compared with the experimental results as shown in Figure 5. The resonance values are very well matched with a slight difference at the anti-resonance impedance which may relate again to the lack of pre-stress in the analytical model. The second peak, near 23 kHz, is the torsional mode of vibration which is extracted from the experimental analysis whilst the analytical model can only predict the longitudinal modes of vibration.

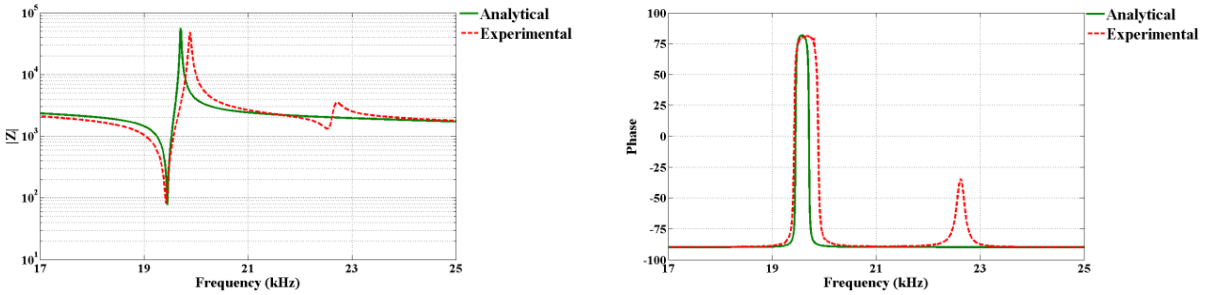

Figure 5. Analytical and experimental impedance spectra (left) and phase-frequency diagram (right).

The electrical currents in the network branches are equivalent to the velocities at the boundaries of the regions, therefore solving for these currents and employing interpolation can allow for calculating the L and T responses along the model as shown in Figures 6(a) and 6(b).

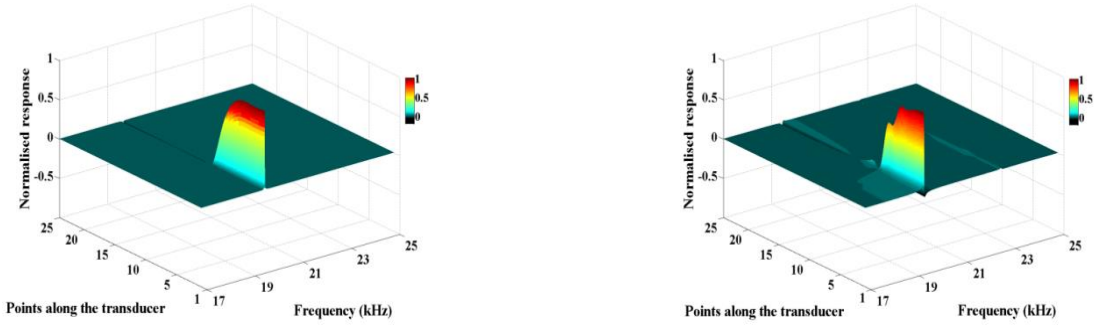

(a)

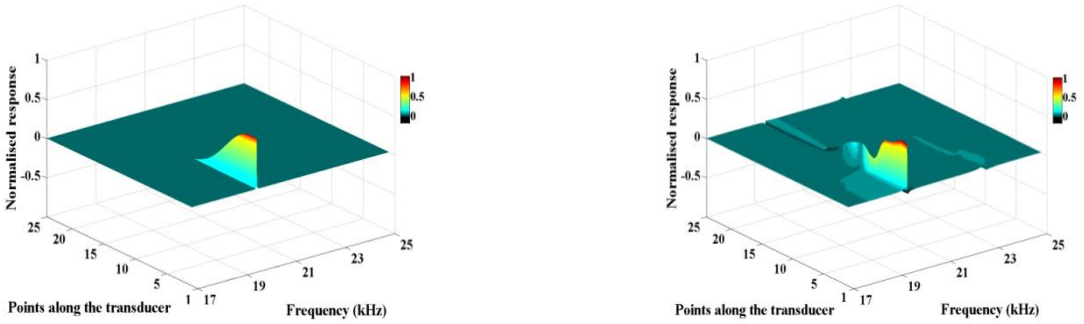

(b)

Figure 6. (a) Analytical (left) and experimental (right) response of L motion along the transducer, (b) analytical (left) and experimental (right) response of T motion along the transducer.

The location of the nodal planes can be found in these figures as the point of change from a positive to negative response. For L responses, the analytical model can predict the location accurately, however, there is a difficulty in locating the T nodal plane because the analytical model does not consider the T wave reflection which produces LT vibration in the piezoelectric and back regions of the transducer model.

Finally, the transducer L and T responses and the input electrical power for different excitation levels are calculated and compared with the experimental results as shown in Figure 7. Good agreement is obtained at lower excitations, however the difference increases at higher excitations as a result of the non-linear increase of mechanical and dielectric loss at higher excitation due to change in the properties of the piezoceramic at elevated temperatures [2].

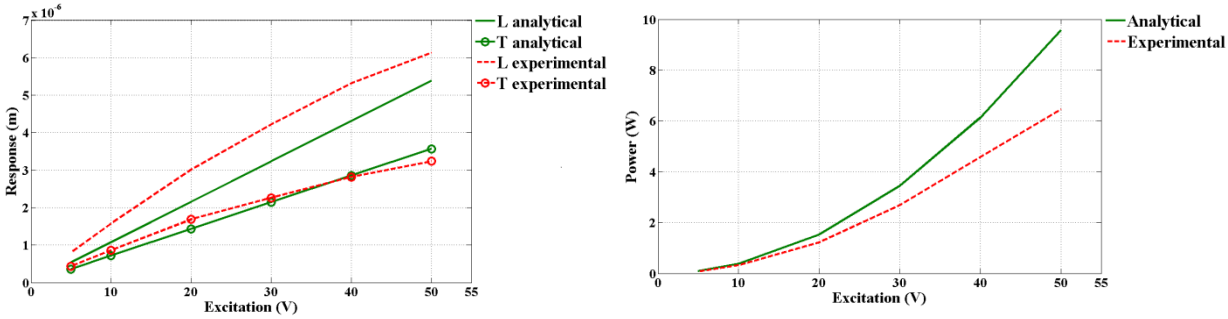

Figure 7. Analytical and experimental L and T responses (left) and electrical input power (right).

5. Conclusions

An analytical model based on the equivalent circuit approach is created for an LT transducer and is used to calculate different electro-mechanical parameters such as resonance and anti-resonance frequencies, coupling coefficient, and the electrical impedance spectrum, the model is also used to locate the nodal plane and to calculate the responses and the input power for different excitation levels. The results show good agreement with experimental findings, with some deficiencies at higher excitation levels.

References

[1] F. Arnold, 2008, Resonance Frequencies of the Multilayered Piezotransducers, *Journal of the Acoustical Society of America,* **123**(5) 3641.

[2] L. Shuyu and T. Hua, 2008, Study on the Sandwich Piezoelectric Ceramic Ultrasonic Transducer in Thickness Vibration, *Journal of Smart Materials and Structures,* **17**(1) 015034.

[3] D. Dragan, D. Mančić and G. Stančić, 2010, New Three-dimensional Matrix Models of the Ultrasonic Sandwich Transducers, *Journal of Sandwich Structures and Materials,* **12**(1) 63-80.

[4] H. Al-Budairi, P. Harkness and M. Lucas, 2011, A Strategy for Delivering High Torsionality in Longitudinal-Torsional Ultrasonic Devices, *Applied Mechanics and Materials,* **70** 339-344.

[5] S. Sherrit, B. Dolgin and Y. Bar-Cohen, 1999, Modeling of Horns for Sonic/Ultrasonic Applications, *Proceedings of the IEEE Ultrasonics Symposium,* **1** 647-651.

[6] W. Mason, 1948, Electromechanical transducers and wave filters, D. Van Nostrand Co., New York.

[7] T. Li, Y. Chen and J. Ma, 2009, Development of a Miniaturized Piezoelectric Ultrasonic Transducer, *IEEE Transactions of Ultrasonics, Ferroelectrics and Frequency Control,* **56**(3) 649-659.

[8] L. Shuyu, 1999, Study on the Longitudinal–Torsional Compound Transducer with Slanting Slots, *Journal of the Acoustical Society of America,* **105**(3) 1643-1650.